

Supplemental information for Parent material and climate interact to control soil C
dynamics through the development of poorly crystalline minerals

Jeffrey Beem-Miller¹, Craig Rasmussen², Alison M. Hoyt^{1,3}, Marion Schrumpf¹, Georg
Guggenberger⁴, & Susan Trumbore¹

¹ Department of Biogeochemical Processes, Max Planck Institute for Biogeochemistry, Jena,
Germany

² Department of Environmental Science, The University of Arizona, Tucson, AZ, USA

³ Department of Earth System Science, Stanford University, Stanford, CA, USA

⁴ Institute of Soil Science, Leibniz University Hannover, Hannover, Germany

Supplemental information for Parent material and climate interact to control soil C dynamics through the development of poorly crystalline minerals

Soil carbon

We did not observe clear trends in soil carbon concentration over time for the majority of sites, making us confident that most sites are at steady-state with regards to carbon stock changes (**Fig. 1**). Although we did observe substantial variation in some sites, this is likely due to spatial heterogeneity in soil C concentration that cannot be avoided when destructively resampling the same sites over time (**Fig. 1**). However, we did observe significant trends in soil C concentration with time for a few of the sites when considered by specific depth increments. However, a caveat here is that we did not account for potential differences in the mass of soil sampled over time, as we only considered depth-based increments. We observed the most significant changes at the soil surface, at three of the 9 sites, but only two sites showed significant changes at the 10-20cm depth, and only one of the soils showed changes at the deepest depth (**Table 1**). The soil at the cold climate andesite site was an outlier in that the soil C concentration showed a consistently significant increase for all depths over the study period (**Table 1**).

Respiration fluxes

SI Figs. 2 and 3.

Radiocarbon depth profiles: 2001 data

Depth profiles of $\Delta^{14}\text{C}_{\text{bulk}}$ were similar in 2001 (**SI Fig. 4**) as to what we observed in 2019. We observed the most depleted ^{14}C overall in the cool climate sites, where we also observed the clearest differences among parent materials. Parent material differences were least apparent for the cold climate sites, as we also observed in 2019. Within climate zones andesitic soils tended be most depleted and the granitic soils most enriched, with the basaltic parent material intermediate between the other two.

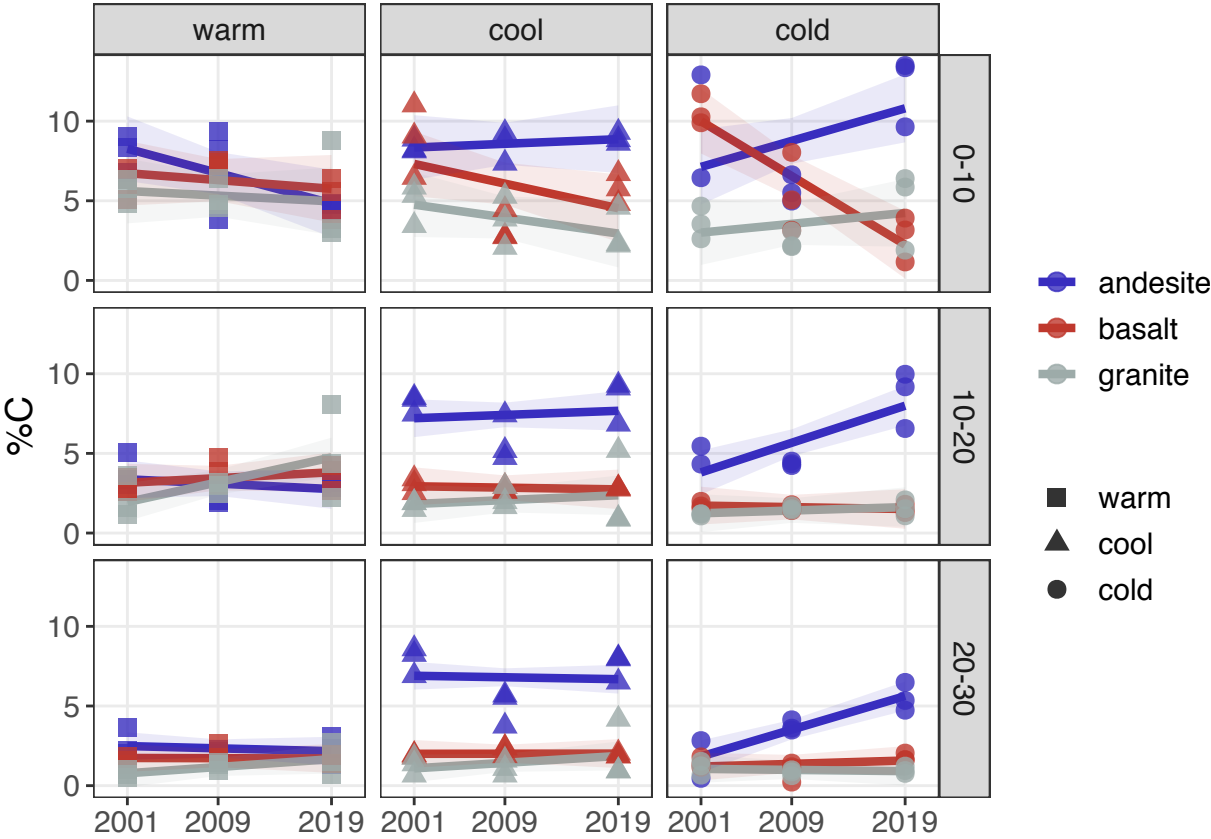


Figure 1. Changes in soil C concentration, 2001-2019. Points show replicate profiles ($n = 3$); lines show marginal mean estimates of linear trends in soil C concentration with time; ribbons show 95% CIs around trend estimates.

Temporal trend analysis

Trends

Please see the main text for discussion of the temporal trends in both $\Delta^{14}\text{C}_{\text{bulk}}$ and $\Delta^{14}\text{C}_{\text{bulk}}$. See SI tables 2 and 3 for statistics.

Contrasts

We saw more significant contrasts for $\Delta^{14}\text{C}_{\text{respired}}$ than we did for $\Delta^{14}\text{C}_{\text{bulk}}$ (SI Fig. 4). When considered within climate zones, the basaltic and granitic soils were more similar to one another overall than were either to the andesitic soils. We observed parent material

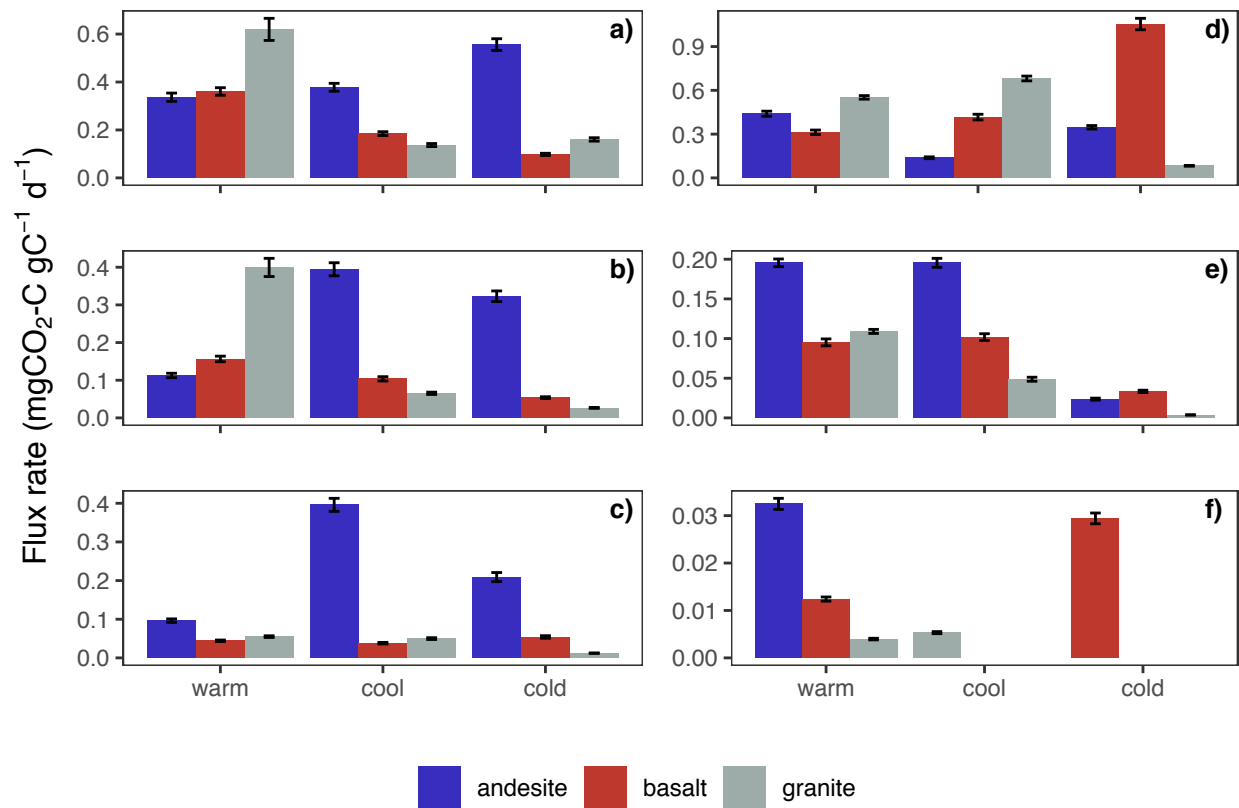


Figure 2. Heterotrophic respiration rates from incubations of 2019 and 2001 samples. Panels a-c show 2019 data, and panels d-f show 2001 data. Panels in the top row (a, d) show the first depth increment for each year, middle row shows the second depth increment (b, e), and the bottom row shows the third depth increment (c, f). Columns show means for laboratory duplicates averaged over the whole incubation period; error bars ± 1 standard error of the mean. NB: Total CO_2 respired was controlled to be within 10,000 ppm ($\pm 1,000$ ppm) for all samples; incubation duration varied between 4 and 40 days.

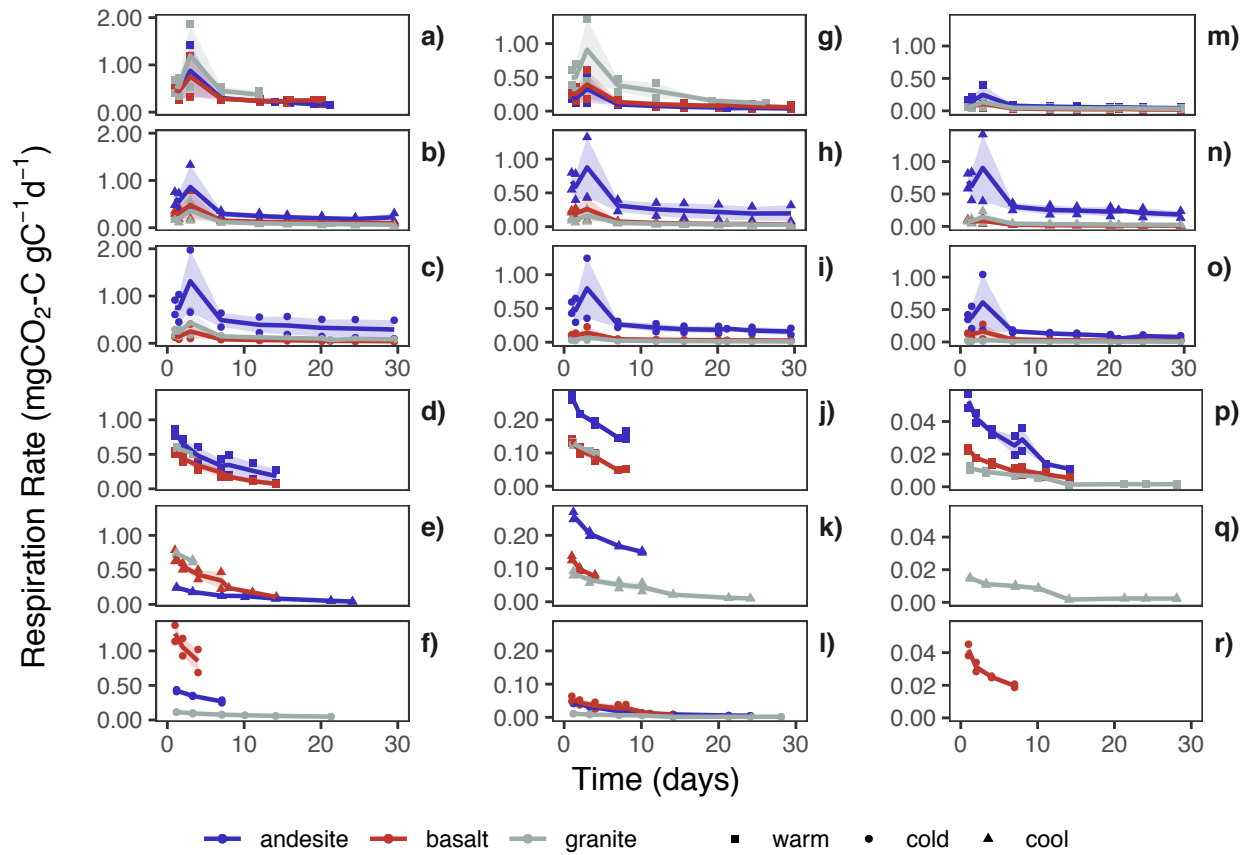


Figure 3. Time series of heterotrophic respiration rates from incubations by depth and year (i.e. samples from the same year and depth interval are plotted on the same scale). Rows correspond to climate zones, columns correspond to depths; leftmost column shows top depth, rightmost column shows deepest depth. Top set of panels (a-c, g-i, and m-o) show 2019 data, bottom set of panels (d-f, j-l, p-r) show 2001 data. Lines show means for laboratory duplicates; ribbon shows minimum and maximum of laboratory duplicates. NB: Total CO_2 respired was controlled to be within 10,000 ppm ($\pm 1,000$ ppm) for all samples.

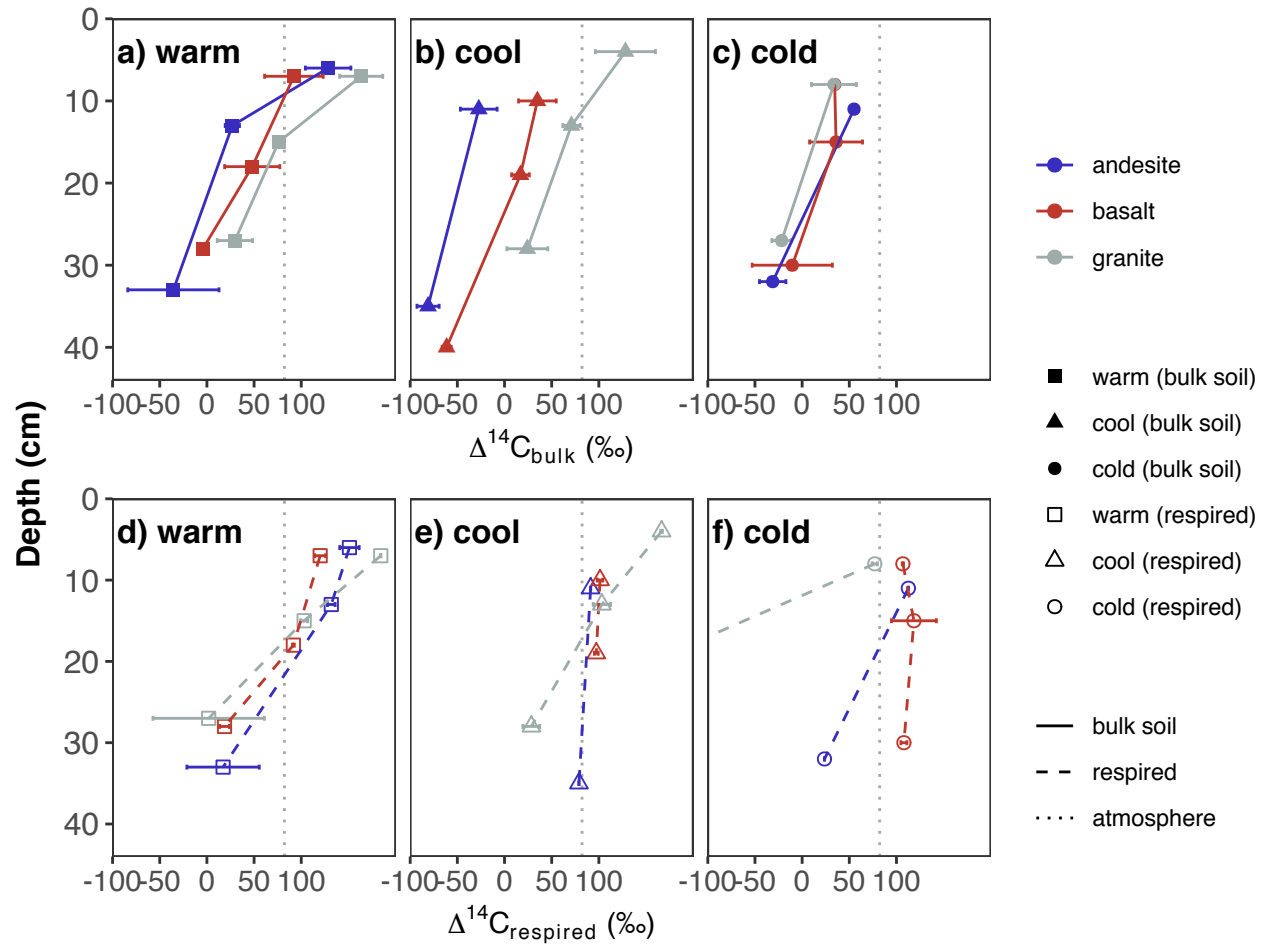


Figure 4. Depth profiles of $\Delta^{14}\text{C}_{\text{bulk}}$ and $\Delta^{14}\text{C}_{\text{respired}}$ for 2001 data. Top panels show bulk data, bottom panels respired data. Panels (a) and (d) show data from the warm climate sites, (b) and (e) from the cool climate sites, and (c) and (f) from the cold climate sites. Dotted vertical lines show $\Delta^{14}\text{C}$ of the atmosphere in the year of sampling. Points show the mean of three replicate profiles for bulk soil, and the mean of laboratory duplicates for respired CO_2 . Error bars show ± 1 SD for bulk soils and the minimum and maximum for respired CO_2 . Respired CO_2 from the cold granite site (panel c) was extremely depleted in $\Delta^{14}\text{C}$ and thus is excluded for display purposes.

contrasts more commonly in the cool and cold climate sites than in the warm sites; however we only observed significant contrasts for the cold climate sites in the $\Delta^{14}\text{C}_{\text{respired}}$ data, and not for $\Delta^{14}\text{C}_{\text{bulk}}$. When considered within parent materials, we saw more significant contrasts for the granitic and basaltic soils than for the andesitic soils (SI Fig. 4).

Mineral assemblages

SI Figs. 5, 6, and 7.

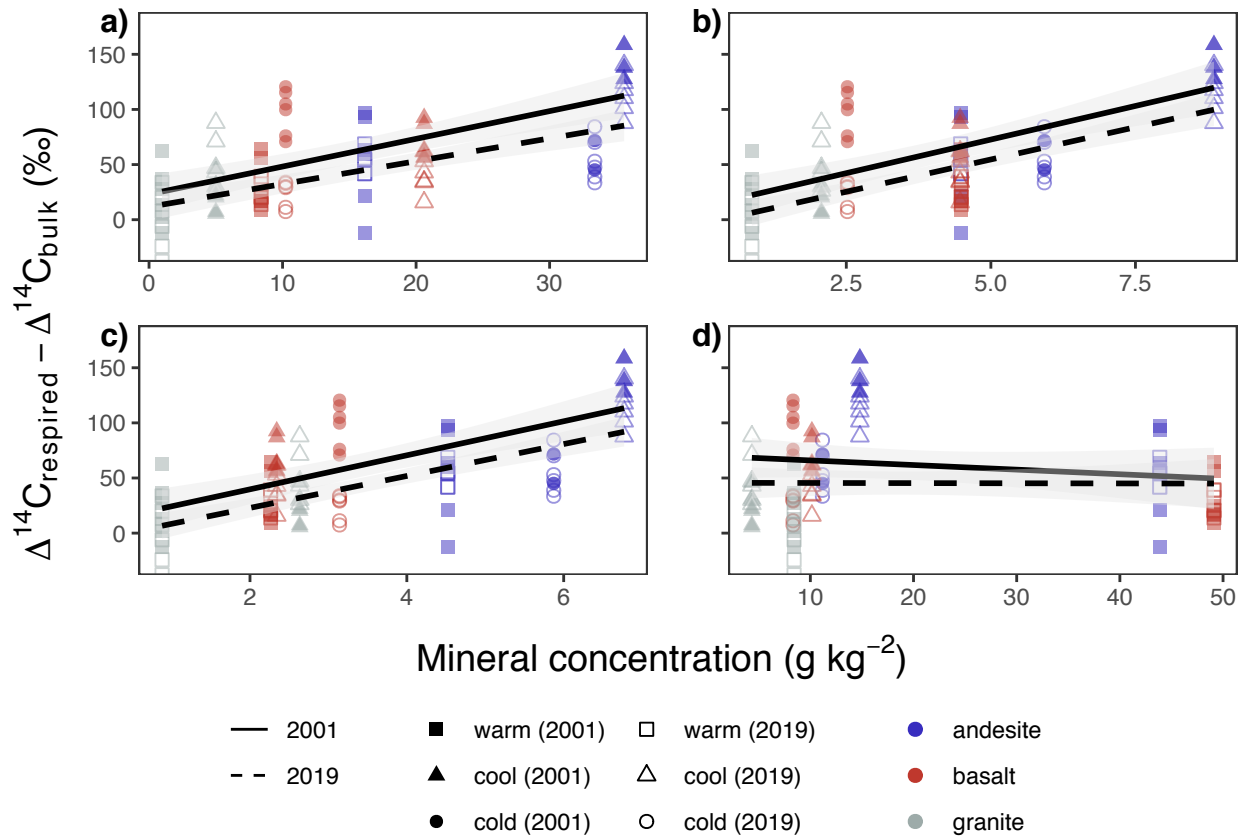


Figure 5. Relationship of selectively dissolved iron and aluminum to the difference between $\Delta^{14}\text{C}_{\text{respired}}$ and $\Delta^{14}\text{C}_{\text{bulk}}$ ($\Delta^{14}\text{C}_{\text{respired-bulk}}$). a) Oxalate-extractable aluminum, b) Pyrophosphate-extractable aluminum, c) Oxalate-extractable iron, d) Dithionite-extractable iron. Points show mass-weighted mineral concentrations and carbon-weighted values of $\Delta^{14}\text{C}_{\text{respired-bulk}}$ for 0-30cm profiles. Lines show linear model fits from Eq. 5.

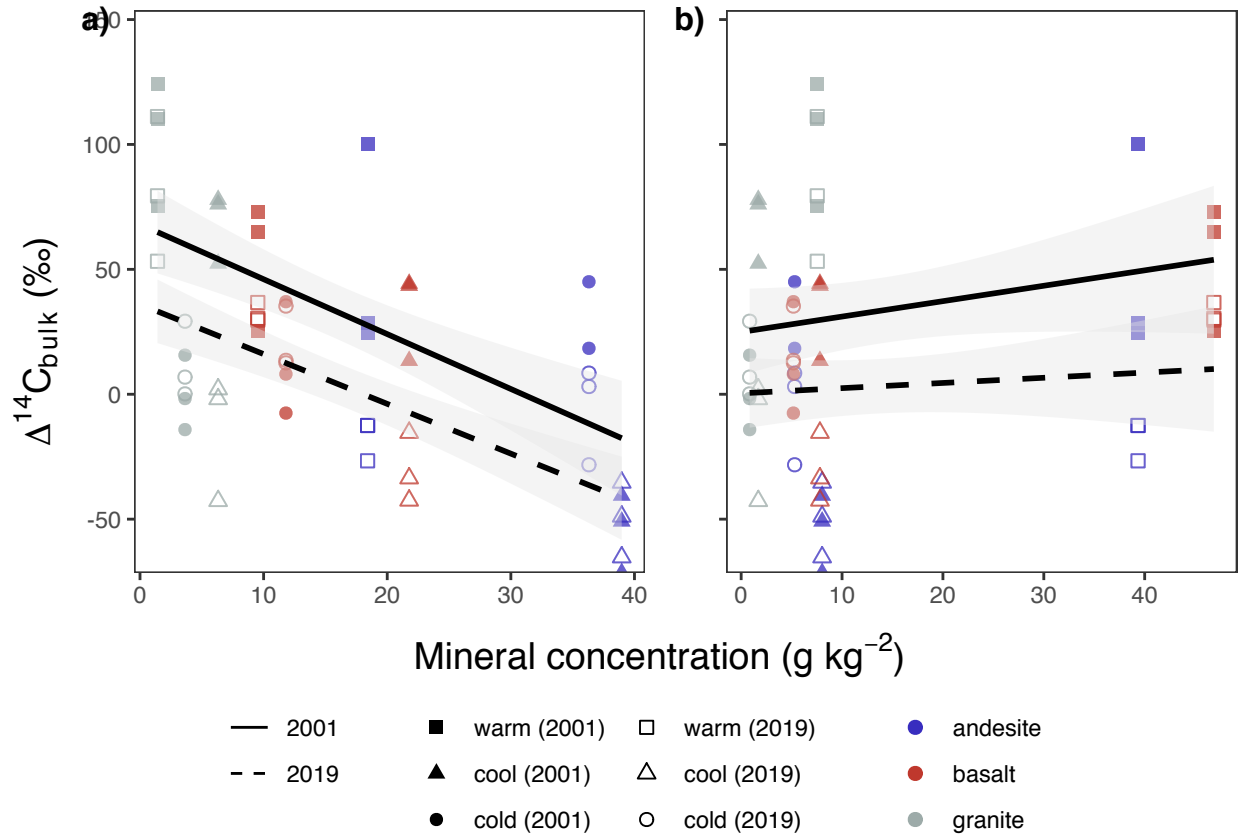


Figure 6. Relationship of poorly crystalline and crystalline minerals to $\Delta^{14}C_{bulk}$. ^{a)} Poorly crystalline mineral content (oxalate-extractable aluminum + 1/2 oxalate-extractable iron), ^{b)} Crystalline mineral content (dithionite-extractable iron - oxalate-extractable iron). Points show mass-weighted mineral concentrations and carbon-weighted values of $\Delta^{14}C_{bulk}$ for 0-30cm profiles. Lines show linear model fits from **Eq. 5**.

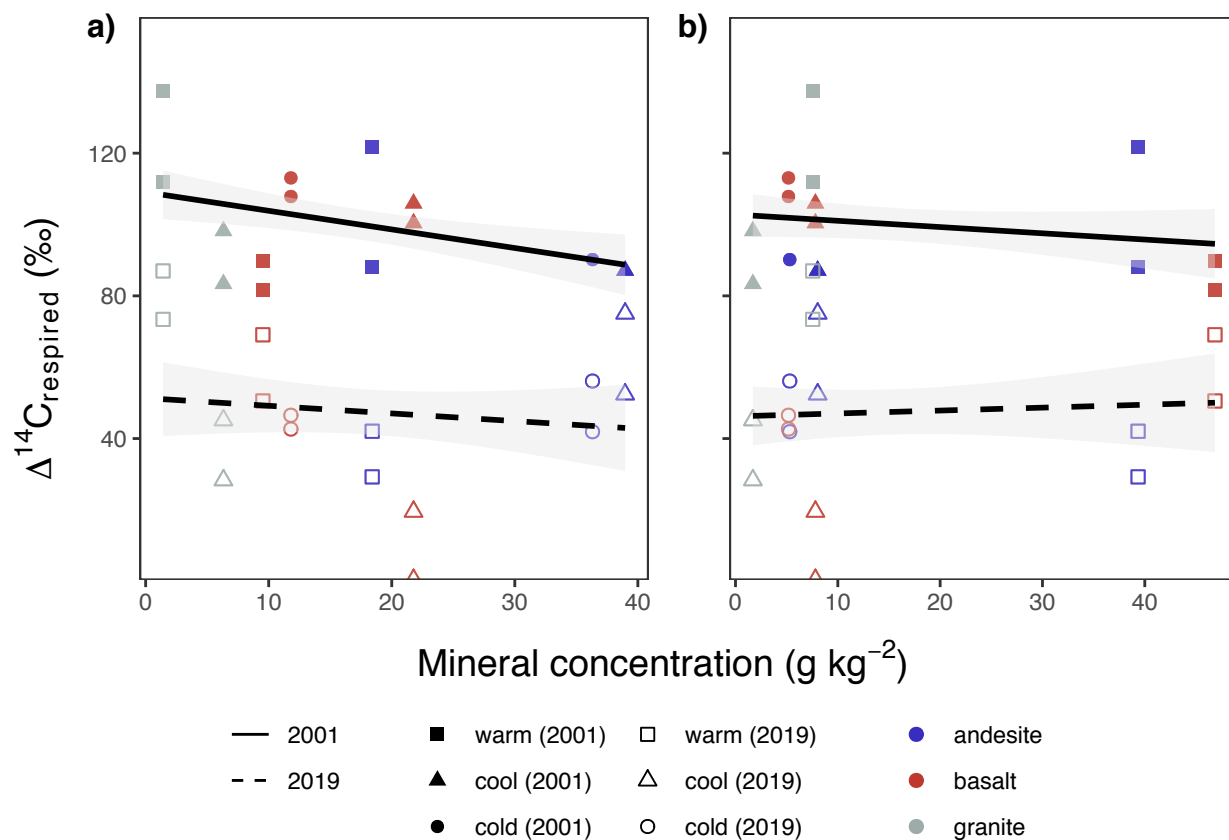


Figure 7. Relationship of poorly crystalline and crystalline minerals to $\Delta^{14}\text{C}_{\text{respired}}$. ^{a)} Poorly crystalline mineral content (oxalate-extractable aluminum + 1/2 oxalate-extractable iron), ^{b)} Crystalline mineral content (dithionite-extractable iron - oxalate-extractable iron). Points show mass-weighted mineral concentrations and carbon-weighted values of $\Delta^{14}\text{C}_{\text{respired}}$ for 0-30cm profiles. Lines show linear model fits from **Eq. 5**.

Table 1

Changes in soil C concentration (%), 2001-2019. (Only significant trends shown).

Depth	Site	Trend	SE	df	95% CI	
					lower	upper
0-10cm	andesite (warm)	-0.19	0.09	62	-0.37	-0.01
	andesite (cold)	0.20	0.10	62	0.01	0.40
	basalt (cold)	-0.43	0.09	62	-0.61	-0.25
10-20cm	andesite (cold)	0.23	0.06	62	0.12	0.35
	granite (warm)	0.16	0.05	62	0.05	0.26
20-30cm	andesite (cold)	0.21	0.04	62	0.13	0.29

Table 2

Change in $\Delta^{14}C_{\text{bulk}}$, 2001-2019. Degrees of freedom = 44; confidence level used = 0.95.

Climate	Parent material	0-10cm		10-20cm		20-30cm	
		Trend	<i>SE</i>	Trend	<i>SE</i>	Trend	<i>SE</i>
warm	andesite	-6.1	1.1	-2.1	1.3	1.1	1.2
	basalt	-1.9	1.1	-0.3	1.3	-1	1.2
	granite	-2.8	1.1	2.1	1.3	0.2	1.2
cool	andesite	0.1	1.1	0.4	1.3	0.3	1.2
	basalt	-2.1	1.1	-3.7	1.3	-6.4	1.2
	granite	-5	1.1	-3.7	1.3	-3.6	1.2
cold	andesite	-2.4	1.2	-1.2	1.4	0.3	1.4
	basalt	0.8	1.1	-0.4	1.3	1.6	1.2
	granite	-0.3	1.1	0.4	1.3	0.3	1.2

Table 3

Change in $\Delta^{14}C_{\text{respired}}$, 2001-2019. Degrees of freedom = 44; confidence level used = 0.95.

Climate	Parent material	0-10cm		10-20cm		20-30cm	
		Trend	<i>SE</i>	Trend	<i>SE</i>	Trend	<i>SE</i>
warm	andesite	-6.2	0.8	-2.3	0.9	1.5	1.7
	basalt	-2.3	0.8	-1.1	0.9	0.5	1.7
	granite	-5	0.8	1.4	0.9	2.8	1.7
cool	andesite	-1.4	0.8	-1	0.9	-1.5	1.7
	basalt	-3.7	0.8	-6	0.9	-7.8	1.7
	granite	-3.1	0.8	-4.3	0.9	0	1.7
cold	andesite	-3	0.8	-1.1	0.9	1.1	1.7
	basalt	-3.8	0.8	-4	0.9	-3.4	2.1
	granite	-0.7	0.8	3.9	1.3	9.3	2.1

Table 4

Contrasts for bulk and respired $\Delta^{14}C$ temporal trends. P value adjustment: Tukey method for comparing a family of 3 estimates.

Depth	Group	Contrast	Bulk			Respired		
			Est.	SE	p	Est.	SE	p
0-10cm	warm	andesite - basalt	-4.2	1.5	0.023	-3.9	1.2	0.009
	warm	andesite - granite	-3.3	1.5	0.091			
	warm	basalt - granite				2.7	1.2	0.08
	cool	andesite - granite	5.0	1.5	0.005			
	cold	basalt - granite				-3.1	1.2	0.037
	andesite	warm - cool	-6.2	1.5	< .001	-4.8	1.2	0.001
	andesite	warm - cold	-3.7	1.6	0.064	-3.3	1.2	0.029
	granite	warm - cold				-4.2	1.2	0.005
	granite	cool - cold	-4.7	1.5	0.01			
10-20cm	warm	andesite - granite	-4.2	1.8	0.055	-3.7	1.3	0.029
	cool	andesite - basalt	4.1	1.8	0.065	4.9	1.3	0.004
	cool	andesite - granite	4.1	1.8	0.068	3.3	1.3	0.055
	cold	andesite - basalt				2.9	1.3	0.097
	cold	andesite - granite				-5.0	1.6	0.015
	cold	basalt - granite				-7.9	1.6	< .001
	basalt	warm - cool				4.8	1.3	0.005
	basalt	warm - cold				2.9	1.3	0.097
	granite	warm - cool	5.8	1.8	0.006	5.7	1.3	0.001
	granite	cool - cold	-4.1	1.8	0.066	-8.1	1.6	< .001

Table 4

Contrasts for bulk and respired $\Delta^{14}C$ temporal trends. P value adjustment: Tukey method for comparing a family of 3 estimates. (continued)

Depth	Group	Contrast	Bulk			Respired		
			Est.	SE	p	Est.	SE	p
20-30cm	cool	andesite - basalt	6.7	1.7	0.001	6.3	2.5	0.054
	cool	andesite - granite	3.9	1.7	0.072			
	cool	basalt - granite				-7.8	2.5	0.016
	cold	andesite - granite				-8.1	2.8	0.025
	cold	basalt - granite				-12.7	3.0	0.002
	basalt	warm - cool	5.5	1.7	0.009	8.3	2.5	0.011
	basalt	cool - cold	-8.0	1.7	< .001			
	granite	warm - cool	3.8	1.7	0.085			
	granite	warm - cold				-6.5	2.8	0.077
	granite	cool - cold	-3.9	1.7	0.072	-9.3	2.8	0.011